

Impact of ocean stratification on submarine melting of a major Greenland outlet glacier

Fiammetta Straneo¹, Ruth G. Curry¹, David A. Sutherland², Gordon S. Hamilton³,
Claudia Cenedese¹, Kjetil Våge⁴, Leigh A. Stearns⁵

¹*Department of Physical Oceanography, Woods Hole Oceanographic Institution, Woods Hole, MA 02543, USA*

²*Department of Physical Oceanography, University of Washington, Seattle, WA 98105*

³*Climate Change Institute, University of Maine, Orono, ME 04469, USA*

⁴*Geophysics Institute, University of Bergen, Norway*

⁵*Department of Geology, University of Kansas, Lawrence, KS 66045, USA*

Submarine melting is an important balance term for tidewater glaciers^{1,2} and recent observations point to a change in the submarine melt rate as a potential trigger for the widespread acceleration of outlet glaciers in Greenland³⁻⁵. Our understanding of the dynamics involved, and hence our ability to interpret past and predict future variability of the Greenland Ice Sheet, however, is severely impeded by the lack of measurements at the ice/ocean interface. To fill this gap, attempts to quantify the submarine melt rate and its variability have relied on a paradigm developed for tidewater glaciers terminating in fjords with shallow sills. In this case, the fjords' waters are mostly homogeneous and the heat transport to the terminus, and hence the melt rate, is controlled by a single overturning cell in which glacially modified water upwells at the ice edge, driving an inflow at depth and a fresh outflow at the surface¹. Greenland's fjords, however, have deep sills which allow *both* cold, fresh Arctic and warm, salty Atlantic waters, circulating around Greenland, to reach the ice sheet margin^{3,6,7}. Thus, Greenland's glaciers flow into strongly stratified fjords and the generic tidewater glacier paradigm is not applicable. Here, using new summer data collected at the margins of Helheim Glacier, East Greenland, we show that melting is driven by both Atlantic and Arctic waters and that the circulation at the ice edge is organized in multiple, overturning cells that arise from their different properties. Multiple cells with different characteristics are also observed in winter, when glacial run off is at a minimum and there is little surface outflow. These results indicate that stratification in the fjord waters has a profound impact on the melting dynamics and suggest that the shape and stability of Greenland's glaciers are strongly influenced by layering and variability in the Arctic and Atlantic waters.

The recent retreat and acceleration of outlet glaciers accounts for 50% of Greenland's net mass loss since 2000⁸. These dynamic changes were initiated at the frontal margins of glaciers grounded hundreds of meters below sea-level in deep, narrow fjords⁹, and coincided with a warming of the waters around Greenland^{10,11}, leading to speculation that an increase in submarine melting was the trigger³⁻⁵. Quantifying ocean-driven melting and identifying its controls on outlet glacier dynamics is thus critical to improving predictions of ice sheet variability and sea level rise.

Submarine melt rates for several Greenland glaciers have been estimated as a residual from mass balance calculations using ice-flow and ice-thickness data^{2,5}. This indirect approach, however, does not provide information on the circulation and water masses responsible for the melting. From the ocean side, the submarine melt rate can, in principle, be estimated from the net oceanic heat transport to the glacier (assuming all the heat is used to melt ice). Yet, obtaining appropriate temperature and velocity measurements to infer the heat transport at the margins of Greenland's glaciers is logistically very challenging. An alternative approach is to assume that the circulation at the ice/ocean boundary consists of a single overturning cell in which a mixture of melt water, run-off and ambient waters rises as a relatively fresh, buoyant plume at the ice/ocean interface, drawing ambient water towards the glacier at depth and driving a fresh outflow at the surface (the 'estuarine circulation'). This widespread paradigm^{5,12,13} is based on observations from Alaskan tidewater glaciers and theories developed for glaciers terminating in a homogeneous fjord¹, as is the case for fjords with shallow sills that allow a single ambient water mass into the fjord. In Greenland, it has been used to estimate submarine melt rates¹² and to explain how variations in the melt rate are

controlled by a limited number of parameters such as, for example, the temperature of the deep oceanic water mass⁵.

An increasing number of surveys of Greenland's fjords have revealed, however, that they contain cold, fresh Arctic waters (PW) *and* warm, salty subtropical waters (STW) from the North Atlantic^{3,6,7} – raising the possibility that submarine melting is driven by more than one water type. Furthermore, laboratory and theoretical studies suggest that the stratification arising from the density contrast between PW and STW may influence the melting process giving rise to a more complex circulation^{14,15} and heat transport than presently envisioned.

Helheim Glacier is a major outlet of the ice sheet in southeast Greenland. Between 2001 and 2005, its terminus retreated ~8 km and its flow speed almost doubled^{16,17}. The glacier terminates in Sermilik Fjord, which is approximately 100 km long, 8 km wide and 600-900 m deep⁷, Fig 1. Surveys conducted in July and September 2008 found that the waters on the shelf, outside Sermilik Fjord, were characterized by a 150 m thick layer of PW overlaying a 500 m thick layer of STW, and that these same waters were present in the fjord beneath a surface layer of glacial water⁷ (GW, a mixture of melt water and run-off). Ice-conditions prevented the 2008 surveys from getting within 50 km of the glacier terminus limiting direct information on the submarine melting process. In August 2009, an ice-breaker and a helicopter were used to conduct a more comprehensive survey of Sermilik Fjord and enabled measurements to be made within 10 km of the terminus [see Methods Section]. A second survey using a small boat and a helicopter [see Methods Section] was conducted in March 2010, when ice-cover in the fjord was incomplete, and reached within 6 km of the terminus, providing the first

measurements of winter conditions in a major glacial fjord in Greenland, Fig 1. These data collectively provide evidence that both water masses contribute to melting, that their layering gives rise to multiple overturning cells, and that these cells vary seasonally, with changes in PW and STW.

Submarine melting is controlled by two factors: 1) thermal forcing of the ambient waters, i.e. the heat available to melt ice, and 2) the circulation at the ice edge¹⁸. Our data suggest that both PW and STW drive submarine melt in summer, when their thermal forcing (i.e. the temperature difference from the freezing point for water of the same salinity and pressure¹⁹), is 2 °C and 5 °C respectively, while in winter only STW drives melting. During winter, STW is actually 1 °C warmer compared to summer, whereas PW is at the freezing point, Fig 2a. Stratification in Sermilik Fjord also exhibits large changes between seasons which could be expected to affect the melting dynamics. In summer, stratification is maximal at the surface due to the GW plume and it decays with depth, Fig 2b and c. In winter, the GW plume is absent, the PW coincides with the winter mixed layer and stratification is large only at the PW/STW interface (~200 m, Fig 2c).

Direct evidence that both STW and PW drive melting is obtained from the temperature and salinity distributions within Sermilik Fjord. Assuming that the surface fluxes are negligible both in summer – when the air-sea fluxes are small and confined to the surface layer – and in winter – when the fjord is mostly insulated by sea ice – the fjord's properties are primarily controlled by the exchanges with the shelf at its mouth and interaction with Helheim Glacier at its head. Near the mouth, rapid fjord/shelf exchanges⁷ tend to restore the fjord's properties to those of the ambient waters on the shelf which, because of their large volume, are unaffected by the glacier. At the ice/ocean

boundary, both submarine melting and run-off from the glacier will cause freshening of the fjord waters and submarine melt will also substantially lower water temperature^{19,20}. Because Sermilik is a narrow fjord, it is not strongly influenced by rotation, and exhibits predominantly along-fjord flows with limited across-fjord variations⁷. Therefore we focus on the property changes in the along-fjord direction.

Along-fjord sections of temperature and salinity show clearly that the PW/STW layering is preserved even in the vicinity of Helheim's terminus (Fig 3 a, b, e, f), supporting the hypothesis that it influences circulation and melting at the ice edge. The complexities of the melting process become evident when one considers the along-fjord changes at a constant depth with respect to conditions close to the mouth of the fjord (we use 30 km, section 3, into the fjord as a reference point, instead of the mouth where temporal variability is much greater and more difficult to characterize). In Figs 3 c, d, g and h, ambient waters modified by glacial processes can be identified by temperature and salinity anomalies which decay away from the glacier, whereas unmodified ambient waters are characterized by zero anomalies. In summer the GW plume emerges very clearly as a cold and fresh anomaly layer near the surface (Fig 3c and g). A separate fresh anomaly is apparent around 200 m (Fig 3g) indicating that some glacially-modified water is flowing out (i.e. away from the glacier) at the PW/STW interface. This intermediate anomaly is warmer than PW and colder than STW (hence the change in temperature anomaly from positive to negative, Fig 3c) which suggests that it consists of a mixture of run off, melt and STW that has upwelled until it encountered its level of neutral buoyancy. This intermediate outflow is also visible in the absolute temperature section (Fig 3a). A third layer of anomalously cold STW water is observed around 500-600 m

(Fig 3c, see also Fig 3a) suggesting an outflow of glacially-modified STW at the bottom of the fjord. By conservation of mass, these outflows must be balanced by inflow in layers characterized by zero anomalies (at 100 m and 400 m). Analysis of the summer data thus reveals the existence of multiple overturning cells (sketched in Fig 3c and g). The existence and structure of the inferred cells are supported by a single velocity profile collected with great effort in summer near the ocean-ice front (see Supplementary Material). Of particular relevance to the heat transport to the ice, our data suggest that much of the heat transport associated with STW is confined beneath the PW/STW.

Multiple overturning cells are also present in winter but with some differences. The GW is generally absent, although a weak, fresh anomaly at the surface suggests the possibility of a thin outflow (Fig 3h). The intermediate outflow at the STW/PW interface is also observed in winter (Fig 3d), but it is saltier than PW (Fig 3h). This difference is likely due to the absence of run off in winter so that the mixture of melt water and STW is saltier than in summer. In winter, a warm anomaly is also observed to reach near the surface, in the proximity of the glacier (Fig 3d). We attribute this to upwelling of a mixture of STW and melt water that is lighter than the winter PW, and speculate that the heat flux associated with this plume can affect sea-ice growth and hence glacier stability. Within the STW layer, anomalies suggest the presence of deeper cells although their circulation appears different from summer (Fig 3d and h).

This analysis confirms that melting is driven by both STW and PW in summer but only by STW in winter. More importantly, it indicates the presence of multiple overturning cells which result in a strongly depth dependent heat transport to the glacier.

This cellular flow pattern is largely consistent with laboratory and theoretical studies of ice melting in a stratified environment^{14,15}.

Potential temperature/salinity (θ/S) characteristics of the fjord waters can be used to distinguish submarine melt from run-off and to support the inferences drawn from the property distribution. From theory, we know that submarine melting will modify the ambient water properties along a particular *melt water line*^{19,20} in θ/S space. The slope of this line in Sermilik Fjord, 2.8 °C/psu, is very close to that of the ambient waters (3°C/psu in summer, and 3.5°C/psu in winter, see Supplementary Material). This means that changes in θ/S driven by melting will closely approximate the ambient water's θ/S line, especially in summer. Thus, the fact that in the waters deeper than 270 m (marked by a Y in Figure 4a-e corresponding to $\theta=2.45$ °C; $S=34.4$; $\sigma_\theta=27.45$ kg/m³), the θ/S slope remains unchanged from the mouth of the fjord to the glacier (Fig 4a-e), even though these waters have become cooler and fresher along that 100 km distance, is consistent with their being modified by submarine melting alone. Shallower than 270 m, on the other hand, the θ/S observed in the vicinity of Helheim departs dramatically from that of the ambient waters (and of the melt water line) indicating that these waters have been modified both by submarine melting and by run off (see Supplementary Material). This is consistent with the conclusion drawn above that the intermediate outflow in summer has been freshened by run off as well as by melting (Fig 3f). It implies that a significant amount of run-off from Helheim is carried by subglacial tunnels to depths of at least 270 m. The signature of run-off is distinctly lacking in the winter profiles for which the θ/S evolution from the mouth toward Helheim transitions quite smoothly from the ambient waters towards the expected melt water line (Fig 4f).

These measurements provide the first evidence that the presence of Arctic and Atlantic waters in Greenland's glacial fjords leads to multiple overturning cells at the ice/ocean interface, giving rise to a non-uniform heat transport and melting with depth. The large density contrast between the two water masses, in particular, constrains the upwelling of modified Atlantic water and hence the vertical transport of heat along the ice. This further suggests that the Atlantic/Arctic interface significantly influences the floating sections of glaciers in Greenland, and that variations in the position of this interface would be expected to affect the glaciers' stability. This adds weight to the possibility that the change in Greenland glacier dynamics over the last decade was not simply a result of the warming the Atlantic waters (estimated to be roughly $1\text{ }^{\circ}\text{C}^{10}$ and hence comparable to the seasonal variation) but also a consequence of the vertical displacement of the Atlantic/Arctic interface due to changes in the large scale ocean circulation.

These results are important for ongoing efforts to understand and quantify the submarine melt rates. They demonstrate clearly that the single overturning cell model (the estuarine circulation model) is not appropriate for Greenland's glaciers and that more sophisticated formulations must be developed which account for ambient stratification. They point out that the Atlantic water temperature alone is likely a poor indicator of the melt rate since other factors, including run-off and melting by Arctic waters, must be considered. Indeed, it is unclear from the existing data whether the submarine melt rates are larger in winter, when the Atlantic waters are warmer, or in summer when the injection of run-off at depth appears to enhance upwelling at the glacier's edge. Sophisticated coupled ocean/glacier models need be developed in conjunction with

process-oriented field and laboratory experiments if we are to be able to resolve the relevant dynamics and, eventually, to provide parameterizations which can be implemented in predictive climate/ice-sheet/ocean models.

Methods Summary

Measurements in Sermilik Fjord in summer 2009 were conducted from the M/V Arctic Sunrise, a class II icebreaker, from August 19th to the 24th. Conductivity, temperature and depth (CTD) profiles were collected at 42 stations using a 6 Hz XR-620 RBR sensor (Fig 1). Water samples were collected at a range of depths and on multiple casts to calibrate the conductivity sensor. Pre- and post-deployment calibrations of the temperature and conductivity sensors were carried out. Bathymetric data were obtained using a 320 Knudsen 12 kHz Echosounder. Two additional temperature and velocity profiles were collected using eXpendable Current Profilers (XCPs) deployed from a helicopter in open water leads in the sea ice.

The winter survey consisted of two expendable CTDs (XCTD) deployed from a small vessel near section 3 on March 15th and three XCTDs and one eXpendable bathythermograph (XBT, recording temperature only) deployed from a helicopter on March 16th, Fig 1. Except for the last XCTD deployed at the mouth, all profiles collected with the expendable probes were cross-calibrated against data collected over the upper 50 m using an RBR XR 620 CTD (deployed either from the boat or from the helicopter).

Supplementary Information accompanies the paper on www.nature.com/nature.

Acknowledgements We thank James Ryder, the entire crew of the M/V Arctic Sunrise and Greenpeace International for their support in making the summer measurements in Sermilik Fjord; J. Kemp and his group for logistic planning of the fieldwork, D. Torres, and S. Worrilow for instrument preparation and support. F.S. acknowledges support from WHOI's Ocean and Climate Change Institute's Arctic Research Initiative and from NSF OCE 0751896, and G.S.H and L.A.S from NASA's Cryospheric Sciences Program.

Authors' Contributions FS, DAS, RGC and GSH conceived the study, F.S., D. A. S., R.G.C, K.V., L. A. S. and G. S. H. participated in the collection of oceanographic data in Sermilik Fjord, and F.S., D. A. S., C.C. were responsible for the analysis and interpretation.

Author Information Correspondence and requests for materials should be addressed to F.S. (fstraneo@whoi.edu).

1. Motyka, R.J., Hunter L., Echelmeyer K.A. & Connor C. Submarine melting at the terminus of a temperate tidewater glacier, LeConte Glacier, Alaska, USA, *Annales Glaciology*, **36**(1), 57-65 (2003).

2. Rignot, E. & Steffen, K. Channelized bottom melting and stability of floating ice shelves. *Geophys. Res. Lett.* **35**, doi:10.1029/2007GL031765 (2008).

3. Holland, D. M., Thomas, R. H., De Young, B., Ribergaard, M. H. & Lyberth, B. Acceleration of Jakobshavn Isbræ triggered by warm subsurface ocean waters. *Nature Geosci.* **1**, 659-664 (2008).

4. Murray, T., Scharrer, K., James, T.D., Dye, S.R., Hanna, E., Booth, A.D., Selmes, N., Luckman, A., Hughes, A.L.C, Cook, S., Huybrechts, P. Ocean-regulation hypothesis for glacier dynamics in south-east Greenland and implications for ice-sheet mass changes. *J. Geophys. Res.*, in press.

5. Motyka, R.J., M. Fahnestock, M. Truffer, J. Mortensen, & Rysgaard, S. Submarine melting of the 1985 Jakobshavn Isbrae floating tongue and the triggering of the current retreat. *J. Geophys. Res.*, under revision.

6. Azetsu-Scott, K. & Tan, F. C. Oxygen isotope studies from Iceland to an East Greenland Fjord: behaviour of glacial meltwater plume. *Marine Chem.* **56**, 239-251 (1997).

7. Straneo, F., G.S. Hamilton, D.A. Sutherland, L.A. Stearns, F. Davidson, M.O. Hammill, G.B. Stenson, and A. Rosing-Asvid, 2010. Rapid circulation of warm subtropical waters in a major, East Greenland glacial fjord. *Nature Geoscience*, **3**, 182-186 (2010).
8. van den Broeke, M., Bamber, J., Ettema, J., Rignot, E., Schrama, E., Jan van de Berg, W., van Meijgaard, E., Velicogna, I., Wouters, B. Partitioning recent Greenland mass loss. *Science*, **326**, 984-986 (2009).
9. Nick, F. M., Vieli, A., Howat, I., M. & Joughin, I. Large-scale changes in Greenland outlet glacier dynamics triggered at the terminus. *Nature Geosci.* **2**, 110-114 (2009).
10. Thierry, V., de Boissésou, E. & Mercier, H. Interannual variability of the Subpolar Mode Water properties over the Reykjanes Ridge during 1990-2006. *J. Geophys. Res.* **113**, C04016, doi:10.1029/2007JC00443 (2008).
11. Myers, P. G., Kulan, N. & Ribergaard, M. H. Irminger Water variability in the West Greenland Current. *Geophys. Res. Lett.* **34**, L17601, doi:10.1029/2007GL030419 (2007).
12. Rignot, E., Koppes M. & Velicogna, I. Rapid submarine melting of the calving faces of West Greenland glaciers, *Nature Geoscience*, **3**, 187-191 (2010).
13. Hanna, E. *et al.* Hydrologic response of the Greenland ice sheet: the role of oceanographic warming *Hydrol. Process.* **23**, 7-30 (2009).

14. Huppert, H.E. and Josberger E.G. The melting of ice in cold stratified water. *Journal of Physical Oceanography* **10**, 953-960 (1980).

15. Huppert, H.E. and Turner, J.S. Ice Block melting into a salinity gradient. *Journal of Fluid Mechanics* **100**, 367–384 (1980).

16. Howat, I. M., Joughin, I. & Scambos, T.A. Rapid changes in ice discharge from Greenland Outlet Glaciers. *Science* **315**, 1559-1561 (2007).

17. Stearns, L. A. & Hamilton, G. S. Rapid volume loss from two East Greenland outlet glaciers quantified using repeat stereo satellite imagery. *Geophys. Res. Lett.* **34**, L05503, doi:10.1029/2006GL028982 (2007).

18. Rignot, E. And Jacobs, S., 2002. Rapid bottom melting widespread near Antarctic ice sheet grounding lines. *Science*, **296**, 2020. Doi: 10.1126/science.1070942.

19. Gade, H.G. Melting of ice in sea water: A primitive model with application to the Antarctic ice shelf and icebergs. *American Meteorological Society*, 189-198 (1979)

20. Jenkins, A. The impact of melting ice on ocean waters. *Journal of Physical Oceanography*, **29**, 2370-2381 (1999)

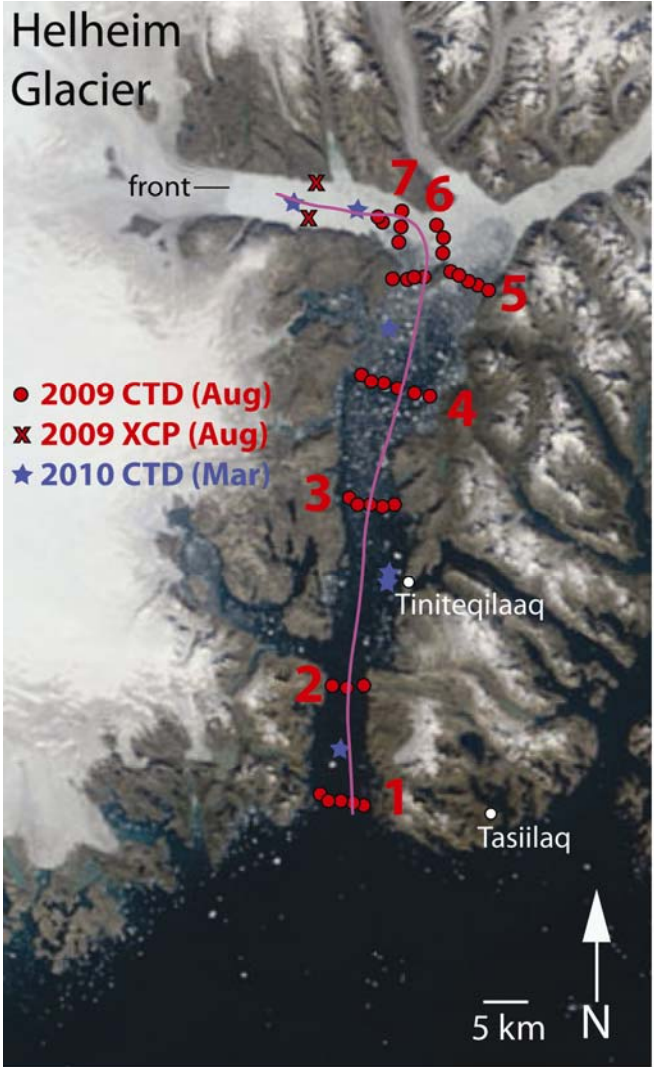


Figure 1: Summer 2009 and winter 2010 surveys of Sermilik Fjord. MODIS image of Sermilik Fjord showing the 2009 and the 2010 station position, including the position of the Helheim's front. The magenta line indicates the along-fjord axis used in Fig 3.

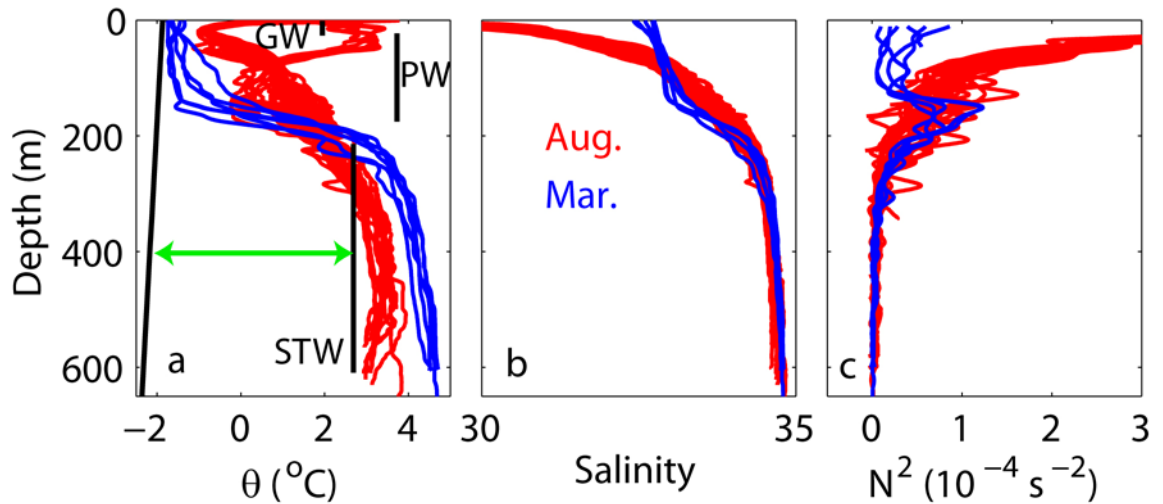


Figure 2. Layering of water masses in Sermilik Fjord. **a)** Potential temperature profiles from August 2009 (red) and winter 2010 (blue). Overlaid in black is the freezing temperature profile with depth for a salinity of 34, representative of the fjord, and the green arrow is the thermal forcing for the summer STW waters. The thickness and vertical position of the STW, PW and GW are also shown (see [Straneo et al 2010] for a definition of the water masses). **b)** Salinity profiles with depth **c)** Stratification profiles with depth expressed as the square of the Brunt-Väisälä frequency.

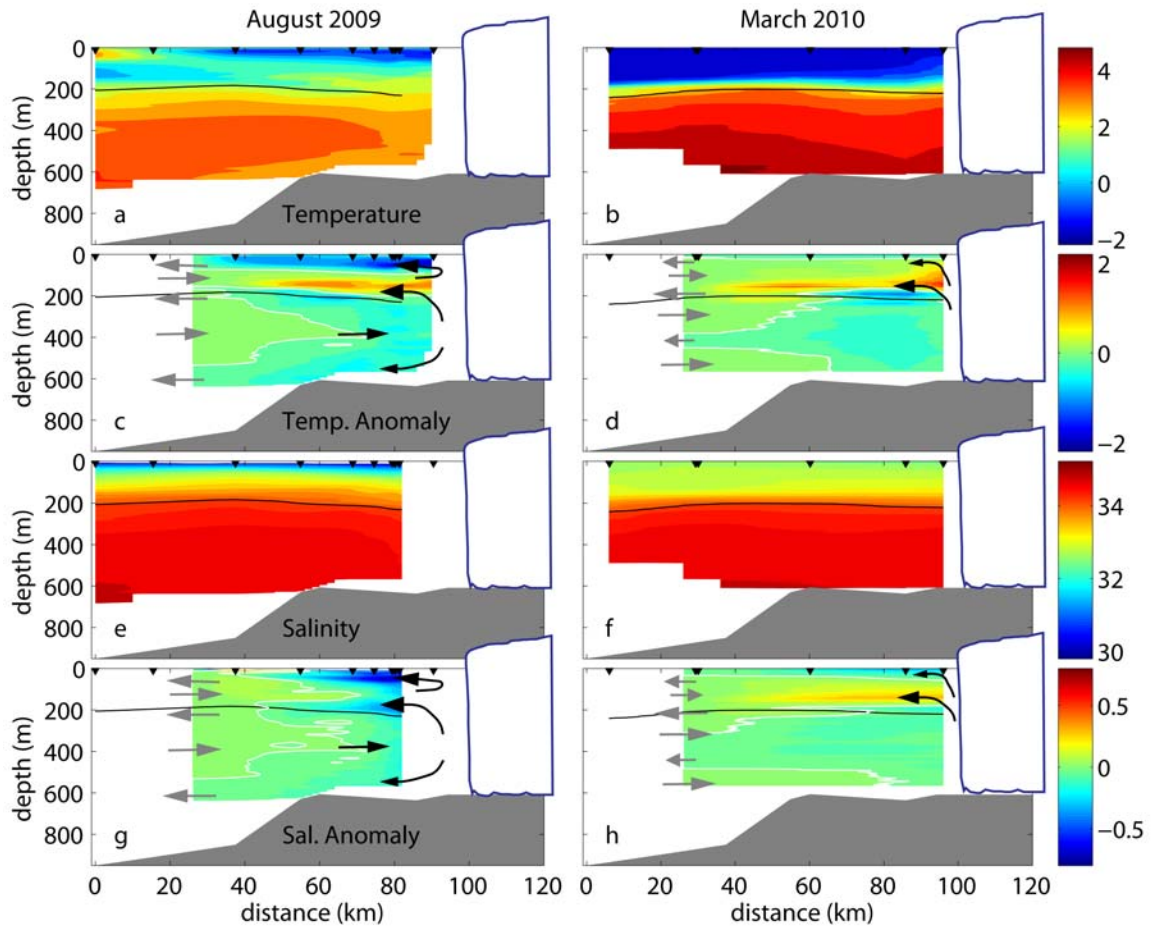


Figure 3 Multiple overturning cells at the edge of Helheim Glacier. **a)** and **b)** Along-fjord potential temperature section in °C for August 2009 and March 2010, respectively; **c)** and **d)** same as a) and b) for the potential temperature anomaly (with respect to distance = 30 km, see text); **e)** and **f)** same as a) and b) but for salinity; **g)** and **h)** same as c) and d) but for the salinity anomaly. The along fjord axis used is shown in Fig 1. For 2009, the along-fjord sections are constructed using an across-fjord averaged profile for each section. The black and gray arrows show the inferred circulation near the glacier and at some distance, respectively (see text). The 34.2 salinity contour, which roughly separates STW and PW, is overlaid in black. Bathymetry shown uses the

maximum depth observed for each section. An idealized schematic of Helheim Glacier is shown in white (blue outline) on all plots.

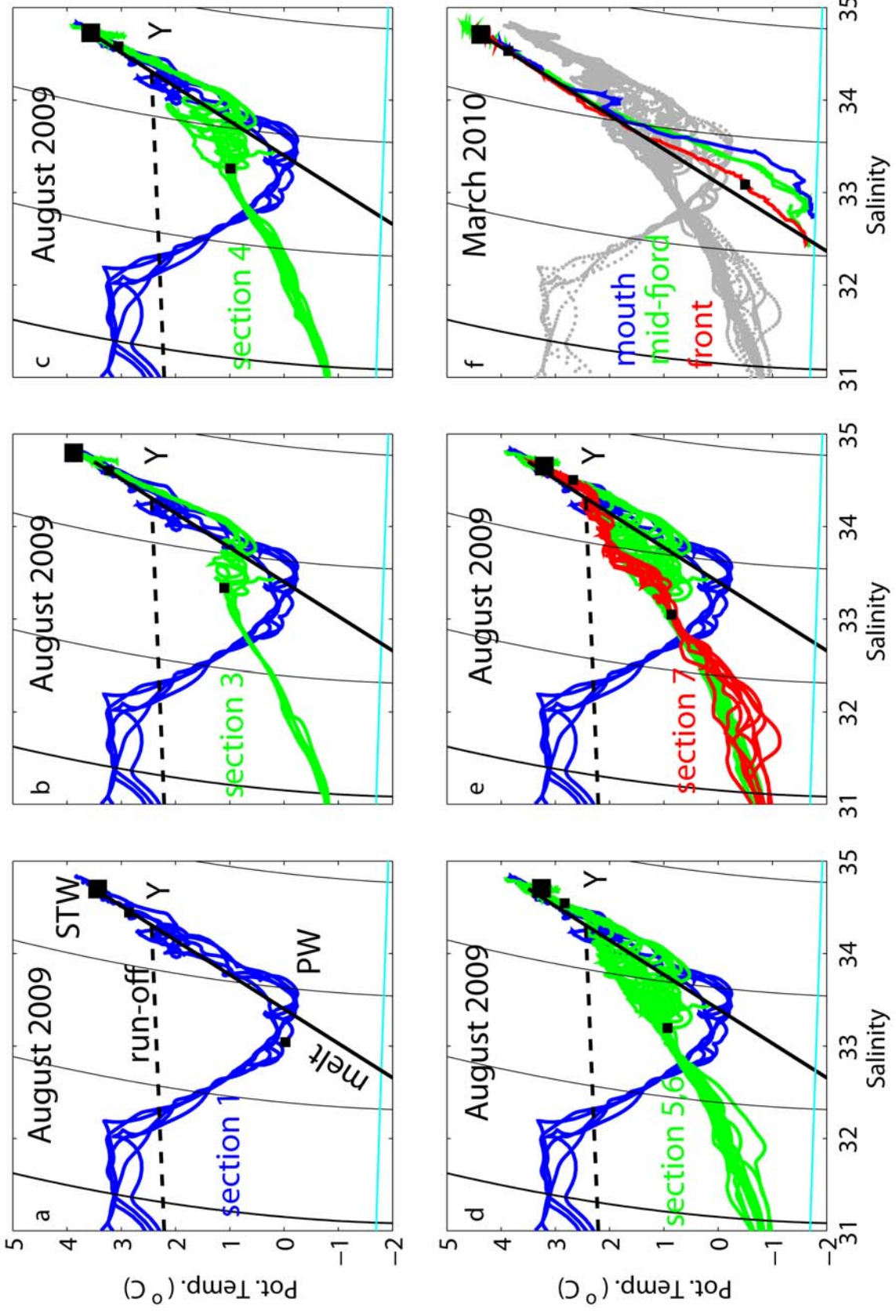


Figure 4 Impact of submarine melt and run-off on the fjord's waters. **a)-e)**

potential temperature/salinity profiles from August 2009. a) shows profiles from the mouth (section1), b) to e) show profiles from progressive sections (see Fig 1) moving towards the head of the fjord. Profiles from the mouth are in blue, from mid-fjord in green and those closest to the front are in red. Overlaid are the melt water line (black solid; uses the densest STW as an end point), the run-off mixing line (black dashed; uses Y as an end point, see Supplementary Material). The θ/S characteristics of PW and STW for August 2009 are shown in a). **f)** θ/S profiles from March 2010, red is the profile closest to the front, blue the one closest to the mouth and green the ones in between. The profiles from August 2009 are superimposed in gray on f) for reference. The melt water line shown uses the winter STW properties as one end point (see Supplementary Material). On all plots a-f, we indicate depth by a large square (500m) and two successive small squares (300m and 100 m) – for the central profile of the section shown. For f) it is for the profiles at the front. Finally the constant density lines are overlaid in black (thin lines), the thickest one to the left indicates $\sigma_{\theta} = 25 \text{ kg/m}^3$, contour interval is 1 kg/m^3 . The line showing the freezing point temperature at the surface is overlaid (cyan).

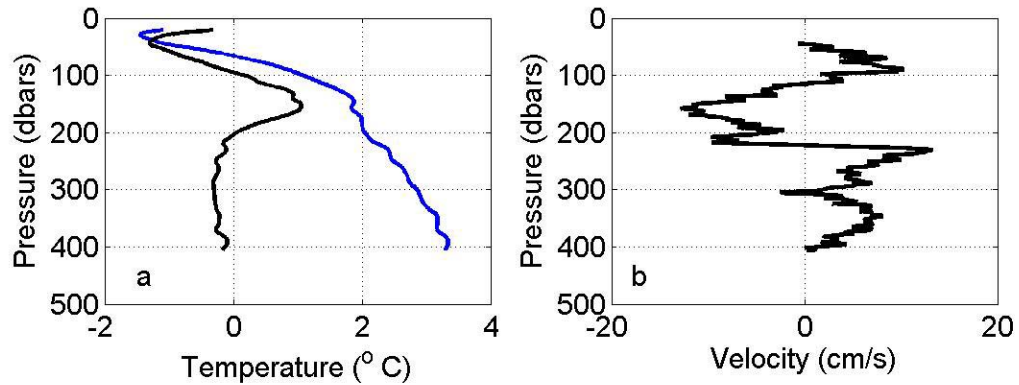
Supplementary Material

1. Circulation in the proximity of Helheim Glacier

Two expendable current profilers (XCP) were deployed in left arm at the head of Sermilik Fjord (known as Helheim Fjord) in August 2009 (Fig 1) and measured velocities as well as temperature as a function of depth. Of the two, only one had velocity errors that were small compared to the observed flows (the errors were likely due to interference of the radio signal with the ice in the fjord). The component of the velocity, from this single profile, oriented along the axis of Helheim Fjord (orientation 105°), and corrected for the magnetic declination (obtained from NOAA's National Geophysics Data Center <http://www.ngdc.noaa.gov>) at the time when the data was collected, is plotted in Supplementary Fig 1, together with the potential temperature profile from the same instrument. Also shown is the potential temperature anomaly between the across-fjord averaged profile at section 3, 30 km into the fjord) and the absolute temperature profile (the same quantity shown in Fig 3c,d) – where a positive anomaly indicates that the waters at the head are warmer than those at 30 km (Supplementary Figure 1a).

The XCP velocity did not provide data for the upper 50m (where the error again was large) and therefore missed the GW plume which flows away from the glacier. Below 50m, however, the profiles show a series of alternating flow directions which agree remarkably well with the direction of flow inferred from the independent measurements of the along-fjord data (see flow sketched in Figure 3c and g). In particular, this velocity profile shows flow away from the glacier at the same depth as the positive temperature anomaly (Supplementary Figure S1a) at the STW/PW interface.

Thus supporting the notion that this melt water/run-off/STW mixture is flowing out at this depth. Beneath this layer, there is evidence of STW flowing towards the glacier.



Supplementary Figure 1: **a)** Potential temperature profile with pressure (blue), from an XCP deployed in August 2009 approximately 11 km from Helheim's front, and potential temperature anomaly profile (black, see text for definition) **b).** Along-fjord velocity (positive is towards Helheim Glacier) from the XCP.

2. Property Transformation as a result of glacial melt and run-off.

i. Slope of the melt water mixing line

Melting of ice lowers both the temperature and salinity of the ambient water. If the ice-ocean system is closed and the ambient water is homogeneous, then the potential temperature/salinity (θ/S) characteristics of the ambient/melt water mixture will fall along a straight *melt water line*¹⁹ in θ/S space, that joins the ambient water's θ/S properties with the ice's θ_{eff}/S , where θ_{eff} is the effective potential temperature of the ice which takes into account that heat is needed to melt ice, and is given by Equation (2) of Jenkins (1999)²⁰:

$$\theta_{\text{eff}} = \theta_f - L/c_p - c_i/c_p(\theta_f - \theta_i)$$

where θ_f is the freezing point temperature of water (which depends on salinity and pressure), L is the latent heat of fusion for ice, θ_i is the actual ice temperature, c_i and c_p are the specific heat capacities of ice and water respectively. If the ambient waters are non-homogeneous but their θ/S characteristics fall on a straight line, then the θ/S properties of the melt water mixture will fall within a triangle defined by the melt water lines characteristic of the two extreme water masses (again if glacial melt is the only process modifying the waters)²⁰.

This second situation applies to Sermilik Fjord where the ambient water consists of a mixture of STW and PW and whose θ/S characteristics fall along the line connecting the θ/S characteristics of the two waters (see mouth profiles in Figure 4a and f). In summer, the characteristic θ/S slope of the ambient water (Supplementary Table 1) is roughly equivalent to the slope for the melt water line estimated according to Jenkins (1999) using an approximate column-averaged ice temperature of -10 °C [cf. Thomas (2004)²¹ for Jakobshavn Glacier in West Greenland], a latent heat of fusion of 334500 J/kg, a specific heat capacity of ice (sea water) of 2100 (3980) J/kg and freezing point temperature of -1.5 °C. (Note that the melt water line slope obtained, 2.8 °C/psu, is not very sensitive to the values of the ice temperature or freezing point temperature chosen.) The similarity of these slopes implies that the predicted triangle reduces to a single line and, furthermore, that the θ/S characteristics of the ambient/melt water mixture will tend to fall on the same line as those of the ambient waters. In winter, the θ/S slope of the ambient waters is not as close as that of the predicted melt water mixing line, implying that one might expect to see the melt water mixture depart from the ambient line.

Supplementary Table 1 – Salinity/Potential temperature characteristics of STW and

PW waters

| | S – STW (psu) | θ - STW (°C) | S – PW (psu) | θ – PW (°C) | θ /S slope ambient (°C/psu) |
|-------------|------------------|------------------------|-----------------|-----------------------|---------------------------------------|
| August 2009 | 34.70 | 3.5 | 33.5 | -0.25 | 3.1 |
| March 2010 | 34.71 | 4.37 | 33.14 | -1.52 | 3.5 |

ii. Melting plus run-off

Similarly to submarine melt, the addition of run-off to ambient water with certain θ /S characteristic will fall along a mixing line whose endpoints are the θ /S of the pure ambient water and $\theta=0$ °C, S=0 (i.e. fresh water at freezing temperature). An example of such a run-off line for ambient waters indicated by point Y is shown in Figure 4a-e. The slope of this ‘run-off’ line tends to be smaller than that associated with submarine melt since for water temperatures characteristic of the polar regions, mixing with run-off has a smaller effect on temperature than melting ice. The run-off line associated with point Y, Figure 3a-e, for example, has a slope of 0.07 °C/psu. A parcel of ambient water which has entrained melt water and run off, then, will have properties which, in θ /S space, fall somewhere in between the run-off and the melt water lines. This is the case for the waters above 270 m in the proximity of Helheim Glacier shown in Figure 4a-e, whose θ /S

characteristics are indicative of a slope of $1.1 \text{ }^{\circ}\text{C}/\text{psu}$, i.e. a value in between the expected melt water and run-off line, Figure 4a-e.

Additional References

21. Thomas, R. H. Force-perturbation analysis of recent thinning and acceleration of Jakobshavn Isbræ, Greenland *J. Glaciol.* **50**, 57-66 (2004).